

## Research Article

# Design, Antileishmanial Activity, and QSAR Studies of a Series of Piplartine Analogues

Flávio R. Nóbrega,<sup>1</sup> Larisse V. Silva,<sup>2</sup> Carlos da Silva M. Bezerra Filho,<sup>1</sup> Tamires C. Lima,<sup>3</sup> Yunierkis P. Castillo,<sup>4</sup> Daniel P. Bezerra ,<sup>5</sup> Tatjana K. Souza Lima,<sup>2</sup> and Damião P. de Sousa <sup>1</sup>

<sup>1</sup>Laboratory of Pharmaceutical Chemistry, Universidade Federal da Paraíba, 58051-900 João Pessoa, PB, Brazil

<sup>2</sup>Department of Cellular and Molecular Biology, Universidade Federal da Paraíba, 58051-900 João Pessoa, PB, Brazil

<sup>3</sup>Department of Pharmacy, Federal University of Sergipe, 49100-000 São Cristóvão, SE, Brazil

<sup>4</sup>Escuela de Ciencias Físicas y Matemáticas, Universidad de Las Américas, Quito, Ecuador

<sup>5</sup>Gonçalo Moniz Institute, Oswaldo Cruz Foundation (IGM-FIOCRUZ/BA), Salvador, Bahia 40296-710, Brazil

Correspondence should be addressed to Damião P. de Sousa; [damião\\_desousa@yahoo.com.br](mailto:damião_desousa@yahoo.com.br)

Received 14 October 2018; Accepted 17 December 2018; Published 8 January 2019

Academic Editor: Andrea Trabocchi

Copyright © 2019 Flávio R. Nóbrega et al. This is an open access article distributed under the Creative Commons Attribution License, which permits unrestricted use, distribution, and reproduction in any medium, provided the original work is properly cited.

Piplartine is an alkamide found in different *Piper* species and possesses several biological activities, including antiparasitic properties. Thus, the aim of the present study was to evaluate a series of 32 synthetic piplartine analogues against the *Leishmania amazonensis* promastigote forms and establish the structure-activity relationship and 3D-QSAR of these compounds. The antileishmanial effect of the compounds was determined using the MTT method. Most compounds were found to be active against *L. amazonensis*. Among 32 assayed derivatives, compound (*E*)-(–)-bornyl 3-(3,4,5-trimethoxyphenyl)-acrylate exhibited the most potent antileishmanial activity ( $IC_{50} = 0.007 \pm 0.008 \mu M$ ,  $SI > 10$ ), followed by benzyl 3,4,5-trimethoxybenzoate ( $IC_{50} = 0.025 \pm 0.009 \mu M$ ,  $SI > 3.205$ ) and (*E*)-furfuryl 3-(3,4,5-trimethoxyphenyl)-acrylate ( $IC_{50} = 0.029 \pm 0.007 \mu M$ ,  $SI > 2.688$ ). It was found that the rigid substituents contribute to increasing antiparasitic activity against *L. amazonensis* promastigotes. The presence of the unsaturated heterocyclic substituent in the phenylpropanoid chemical structure (furfuryl group) resulted in a bioactive derivative. Molecular simplification of benzyl 3,4,5-trimethoxybenzoate by omitting the spacer group contributed to the bioactivity of this compound. Furthermore, bornyl radical appears to be important for antileishmanial activity, since (*E*)-(–)-bornyl 3-(3,4,5-trimethoxyphenyl)-acrylate exhibited the most potent antileishmanial activity. These results show that some derivatives studied would be useful as prototype molecules for the planning of new derivatives with profile of antileishmanial drugs.

## 1. Introduction

Leishmaniasis is a tropical disease prevalent in 98 countries and has high impact on South America, Africa, and Asia (especially India). This illness is caused by protozoan parasites of the *Leishmania* genus and is transmitted to humans by the bite of infected female phlebotomine sandflies. There are at least twenty species of *Leishmania* that cause clinical manifestations in humans, and they can occur in three different forms: (i) visceral leishmaniasis, (ii) cutaneous leishmaniasis, and (iii) mucocutaneous leishmaniasis. The most severe form is visceral leishmaniasis, characterized by prolonged fever, hepatomegaly, splenomegaly, substantial

weight loss, and progressive anemia, and if left untreated, it can be fatal in 95% of cases [1–3].

The drugs currently available for treatment of leishmaniasis are pentavalent antimonials glucantime, bisamidines (pentamidine and stilbamidine), miltefosine, and amphotericin B. Unfortunately, all these drugs have several limitations, such as low efficacy, toxicity to the liver and heart, elevated cost, and parasite resistance. For these reasons, new and more efficient therapeutic approaches are needed for prevention and treatment of leishmaniasis [1]. Natural products provide a virtually unlimited source of inspiration for new, powerful and selective drug leads. It is estimated that 20,000 plant species have antiparasitic

activities. A wide variety of secondary metabolites have antileishmanial activity, namely, alkaloids, triterpenes, terpenoids, chalcones, saponins, glycosides, acetogenins, and flavonoids [4–6].

Piperaceae family, also known as pepper family, comprises over 1,000 species distributed pantropically. The *Piper* genus is the most diverse of the Piperaceae family and produces a number of structural classes (lignans, phenylpropanoids in the form of amides, and other derivatives of phenylpropanoids) with several biological activities, including antileishmanial activity [7–9]. In a study [7], antileishmanial activity of *n*-hexane, ethyl acetate, acetone, and methanol extracts from *Piper cubeta* fruits and *Piper retrofractum* stem bark was investigated against *Leishmania donovani* promastigotes. Among these substances, pipartine demonstrated the highest leishmanicidal activity, with an  $IC_{50}$  value of  $7.5 \mu M$ . Furthermore, this molecule was 3 times more potent than positive control pentamidine ( $IC_{50} = 25 \mu M$ ) [7, 8].

Piplartine (**1**) (Figure 1), also known as piperlongumine, is an alkamide found in large quantities in long pepper (*Piper longum* L.). In addition to antileishmanial and trypanocidal activities, this alkamide has been also reported as having other pharmacological activities, including antitumor, cytotoxic, antinociceptive, antiplatelet aggregation, and antimetastatic activities [10]. Thus, the goals of the present study were to synthesize a series of 32 pipartine analogues and evaluate the structure-activity relationship among these derivatives against *Leishmania amazonensis* promastigotes.

## 2. Results and Discussion

**2.1. Chemistry and Antileishmanial Activity of Compounds 5–36.** For this study, a series of 32 analogues of **1** (Scheme 1) were synthesized, preserving the (*E*)-3-(3,4,5-trimethoxyphenyl)-acryloyl moiety on cinnamic esters and amides and changing this moiety on benzoic esters by removing the ethylene group between carbons 2 and 3. Side-chain modifications were also evaluated changing the radical *R* to methyl (**5**), ethyl (**6**), propyl (**7**), *i*Pr (**8**), butyl (**9**), pentyl (**10**), decyl (**11**), 2-methoxyethyl (**12**), 4-methoxybenzyl (**13**), phenylethyl (**14**), 4-methylphenylethyl (**15**), carvacryl (**16**), CHPh<sub>2</sub> (**17**), furfuryl (**18**), eugenyl (**19**), (–)-bornyl (**20**) and piperonyl (**21**) on cinnamic esters, and butyl (**22**), *N,N*-diethyl (**23**), octyl (**24**), cyclohexyl (**25**) benzyl (**26**), pyrrolidyl (**27**), 4-methylbenzyl (**28**), 4-methoxybenzyl (**29**), 4-fluorobenzyl (**30**), 4-chlorobenzyl (**31**), 4-bromobenzyl (**32**), 2,4-dimethoxybenzyl (**33**), and 3,4-dimethoxybenzyl (**34**) on amides. The benzoic esters synthesized were 2-methoxyethyl-3,4,5-trimethoxybenzoate (**35**) and benzyl 3,4,5-trimethoxybenzoate (**36**) [8–12].

To synthesize the analogues, the following starting materials were used: 3,4,5-trimethoxycinnamic acid (**2**); 3,4,5-trimethoxybenzoic acid (**3**); 3',4',5'-trimethoxyacetophenone (**4**); and ROH to esters and primary or secondary amines to amides. Most products were obtained in high yields, and the reactions (a, b, c, d, e, and f) were performed in one step (Scheme 1).

The antileishmanial potential of all pipartine analogues (**5–36**) against the strains IFLA/BR/1967/PH8

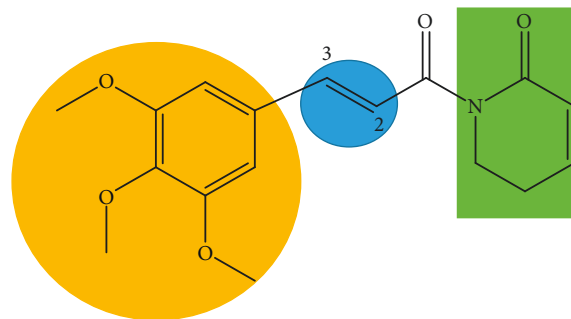


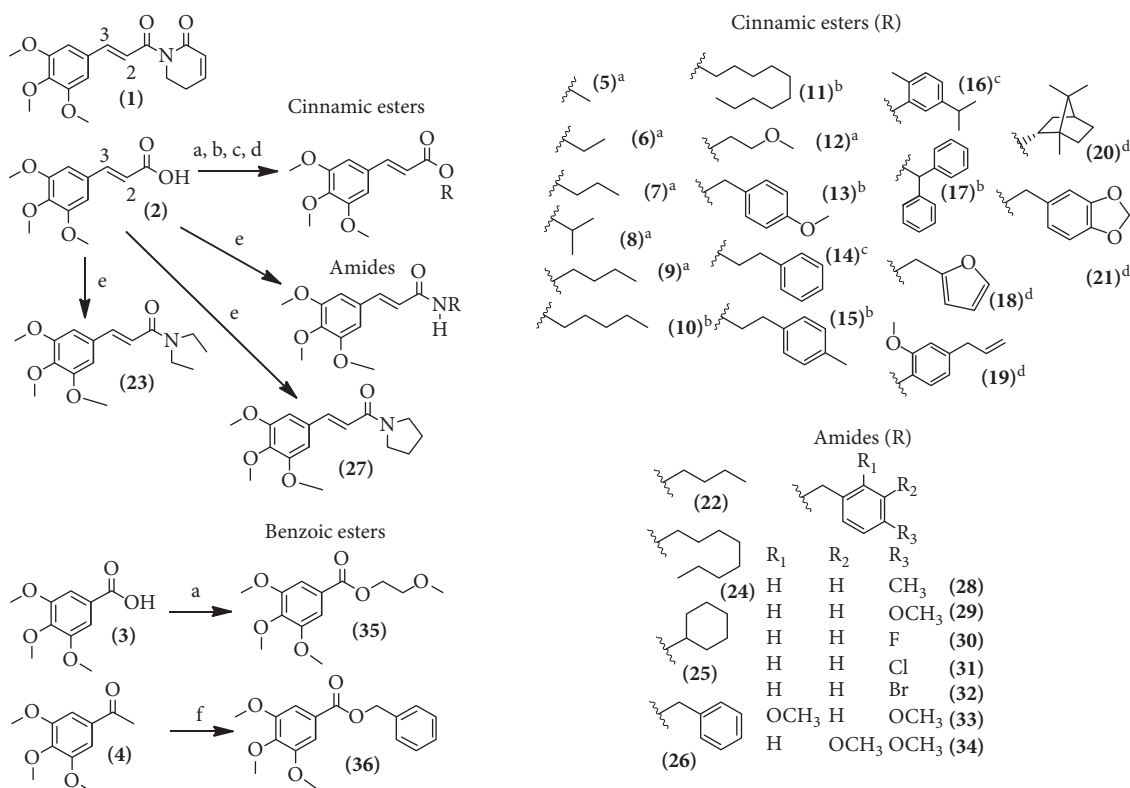
FIGURE 1: Chemical structure of pipartine (**1**). Modifications in the green and blue substructures of the molecule were investigated in the present study.

*L. amazonensis* was evaluated using the MTT method. The experiments were performed against promastigote forms, that is the proliferative form found in the invertebrate host, and the tests compounds were assayed at following concentrations: 3.125, 6.25, 12.5, 25, 50, 100, 200, and 400  $\mu g/ml$ . The antileishmanial activity was assessed as  $IC_{50}$  and expressed in  $\mu M$ .  $IC_{50}$  values of the pipartine analogues are summarized in Table 1.

Most compounds tested against the promastigote forms of *L. amazonensis* were bioactive (**6–13**, **15**, **17**, **18**, **20**, **21**, **23**, **25**, **27**, **28**, and **36**). Among the 32 assayed derivatives, compound **20** ( $IC_{50} = 0.007 \pm 0.008 \mu M$ ) exhibited the best antileishmanial activity, followed by **36** ( $IC_{50} = 0.025 \pm 0.009 \mu M$ ), **18** ( $IC_{50} = 0.029 \pm 0.007 \mu M$ ), and **21** ( $IC_{50} = 0.042 \pm 0.011 \mu M$ ). For compounds **31**, **33**, and **34**, their  $IC_{50}$  cannot be determined. Amphotericin B, standard drug, exhibited an  $IC_{50}$  value of  $0.0015 \mu M$ .

The statistical parameters of the obtained 3D-QSAR model as well as superposition of the 3D structures from which it was derived are summarized in Figure 2. In this figure are also presented the general scaffold of the compounds under study, the plot of the predicted vs. observed  $pIC_{50}$  values for the training set, and the results of LOO cross-validation procedures. The obtained statistical parameters show that the developed model is accurate and robust. This is supported by the high values of  $q^2$  obtained during the LOO and LMO cross-validation experiments. Regarding the influence of the steric and electrostatic factors on bioactivity, it was found that both contribute almost equally to explain the observed bioactivity.

In general, compounds containing O in the X position (see Figure 2) were more active than those containing NH at the same position. This effect can be clearly observed for compounds **17** and **23** whose only difference is the presence of NH (**17**) vs. O (**23**) at position X, compound **23** being 6.5-fold more active than **17**. This can be due to electrostatic fields surrounding this position, as shown in Figure 3(a). These fields indicate that negatively charged substituents are favored at position X, which is the case of the compounds with O at this position. This observation can be generalized to all the compounds in the dataset. A special case is compound **29** that lacks the double bond spacer. In terms of electrostatic potential, the O atom at the X position remains close to the electronegative field while the lack of the spacer



SCHEME 1: Synthesis method: (a) ROH, H<sub>2</sub>SO<sub>4</sub>, reflux; (b) Et<sub>3</sub>N, RBr or RCl, acetone, reflux; (c) SOCl<sub>2</sub>, reflux (d) DCC, DMAP, CH<sub>2</sub>Cl<sub>2</sub>, r.t.; (e) RNH<sub>2</sub>, (CH<sub>3</sub>CH<sub>2</sub>)<sub>2</sub>NH or pyrrolidine, BOP, Et<sub>3</sub>N, CH<sub>2</sub>Cl<sub>2</sub>, DMF; (f) ROH, CuBr, pyridine, chlorobenzene, BF<sub>3</sub>·O(Et)<sub>2</sub>.

TABLE 1: Antileishmanial activity of compounds 5–36 against the strains IFLA/BR/1967/PH8 of *Leishmania (L.) amazonensis*.

Cinnamic esters		Amides		Benzoic esters				
	IC <sub>50</sub> (μM)	SI	IC <sub>50</sub> (μM)	SI	IC <sub>50</sub> (μM)	SI		
5	0.641 ± 0.052	>0.154	22	0.577 ± 0.080	>0.148	35	>0.656 ± 0.05	>0.141
6	0.257 ± 0.041	>0.364	23	0.091 ± 0.015	>0.126	36	>0.02 ± 0.0	>3.205*
7	0.09 ± 0.032	>0.992	24	0.564 ± 0.061	>0.126			
8	0.194 ± 0.04	>0.459	25	0.117 ± 0.027	>0.678			
9	0.149 ± 0.025	>0.570	26	0.734 ± 0.252	>0.104			
10	0.133 ± 0.014	>0.608	27	0.353 ± 0.080	>0.243			
11	0.076 ± 0.009	>0.868	28	0.109 ± 0.010	>0.063			
12	0.076 ± 0.022	>1.106	29	0.662 ± 0.188	>0.105			
13	0.101 ± 0.031	>0.688	30	1.137 ± 0.252	>0.062			
14	0.975 ± 0.241	>0.069	31	>1.108	>0.062			
15	0.125 ± 0.035	>0.561	32	0.486 ± 0.043	>0.127			
16	0.513 ± 0.065	>0.142	33	>1.033	>0.062			
17	0.083 ± 0.016	>0.748	34	>1.033	>0.062			
18	0.029 ± 0.007	>2.688*						
19	>1.041	>0.062						
20	0.007 ± 0.008	>10*						
21	0.042 ± 0.011	>1.582	-					
				Positive control: amphotericin B		0.0015		

\*Cytotoxic effects on MRC5 (Medical Research Council cell strain 5—fibroblast derived from lung tissue); positive control: doxorubicin (IC<sub>50</sub> 0.00287 (0.0017–0.0050) μM). SI: selectivity index.

places the trimethoxyphenyl group in a region where an electronegative MIF is present. Thus, compounds without the spacer will have higher bioactivity compared to those containing the double bond spacer. Finally, the electro-positive potential observed around position *R* correlates with

the favorable influence of aromatic substitutions at this position.

We also analyzed the influence of the steric molecular interaction fields. These fields are summarized in Figure 3(b), and it can be seen that the substituents attached

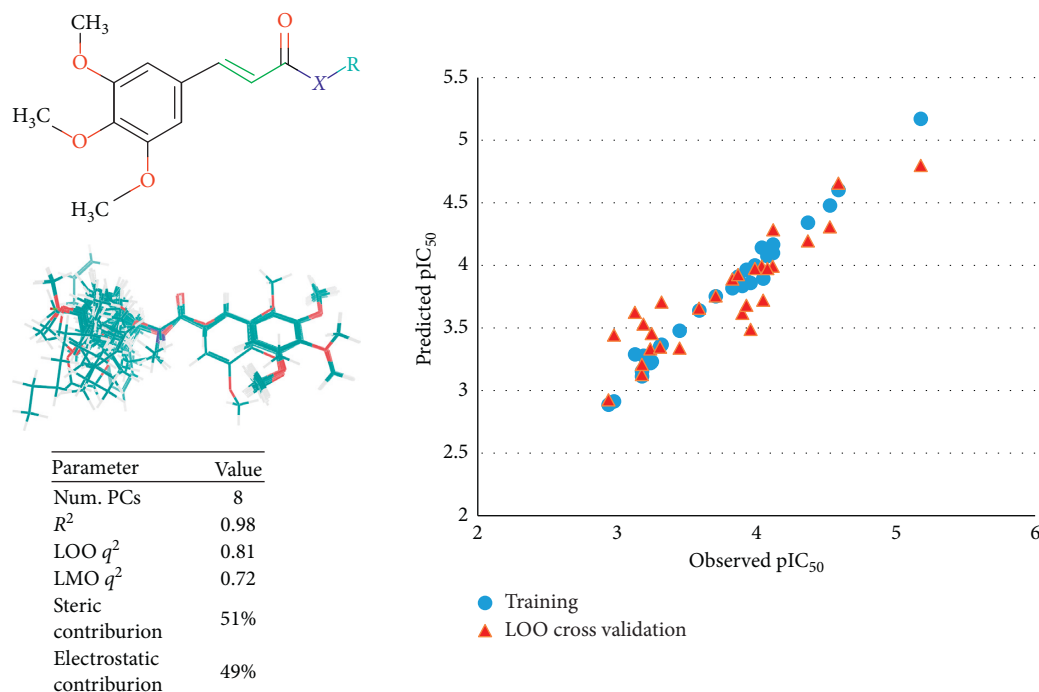


FIGURE 2: Summary of the QSAR modeling procedure.

to the *R* position are surrounded by a steric favorable region beyond which a steric unfavorable potential is located. In consequence, bulky substituents at *R* are favorable for bioactivity. *Para*-substituted phenyl rings are tolerated, whereas *meta*- and *ortho*-substituted rings decrease bioactivity. The steric effect for different groups at *R* is depicted in Figure 3(c) for compounds **27**, **10**, and **21**.

From Figure 3, it can be seen that compound **27** lies entirely within the steric favorable region, while compounds **10** and **21** bear substituents which protrude into the unfavorable steric region. In addition to **27**, the other two most active compounds (**29** and **25**) are also substituted at *R* with groups completely falling within the steric favorable region. On the other hand, large substituents such as those present in compounds **9** and **26** reach the steric unfavorable region, which reduce their bioactivity. To avoid falling within the steric unfavorable region, if rings are used at *R*, no more than one methyl group should link them to *X*. Furthermore, nonbulky groups at *R* such as aliphatic substitutions lead to nonoptimal bioactivity because of their inability to completely occupy the steric favored region. The structure-activity relationship (SAR) derived from these analyses is summarized in Figure 3(c).

**2.2. Anti-Leishmania Activity of Compounds 5–36.** Pentavalent antimonials, in use for more than six decades, are still the first-line of treatment for visceral leishmaniasis, also known as kala-azar black fever. However, this therapeutic option presents several limitations, including side effects, the need for daily injections, and drug resistance, and requires a long treatment regimen. Thus, developing and testing of new compounds with leishmanicidal activity is of

paramount importance to improve disease treatment and control. Several medicinal plant secondary metabolites have shown interesting antileishmanial activities, including alkaloids, steroids, terpenoids, phenolic acids, and phenylpropanoids [13–15].

The chloroform extract of *Valeriana wallichii* rhizomes was investigated to identify the structures responsible for its antileishmanial activity. A bioassay-guided fractionation was undertaken and resulted in (–)-bornyl caffeate,  $\alpha$ -kessyl alcohol, two cinnamic acid derivatives, and four valtrates. All these compounds exhibited antileishmanial activity against *L. major* promastigotes, with IC<sub>50</sub> values varying between 0.8 and 48.8  $\mu$ M. Furthermore, some compounds were more potent than the positive control miltefosine (IC<sub>50</sub> = 36.2  $\mu$ M) [16].

A phytochemical study guided by the antileishmanial activity of the crude extract from the stem bark of *Tecoma mollis* yielded seven phenylpropanoid glycosides. These secondary metabolites were tested against the promastigote forms of *L. donovani*, and pentamidine and amphotericin B were used as positive controls. The compounds acteoside, luteoside A, and luteoside B shared the highest IC<sub>50</sub> values: 30.08, 15.07, and 6.71  $\mu$ g/ml, respectively. The IC<sub>50</sub> values of the positive controls were 0.34  $\mu$ g/ml to amphotericin B and 1.31  $\mu$ g/ml to pentamidine. The obtained results also revealed that *ortho*-dihydroxy phenyl group (catechol moiety) was important to the antileishmanial activity [17].

Piplartine (**1**), a plant metabolite, is classified as an alkamide and contains in its structure a 3,4,5-trimethoxycinnamic acid (**2**) moiety and a  $\delta$ -lactam ring. Both **1** and **2**, used as starting materials to synthesize some piplartine analogues, were tested against IFLA/BR/1967/PH8 *L. amazonensis*. The IC<sub>50</sub> values found were  $179 \pm 0.05$   $\mu$ g/ml

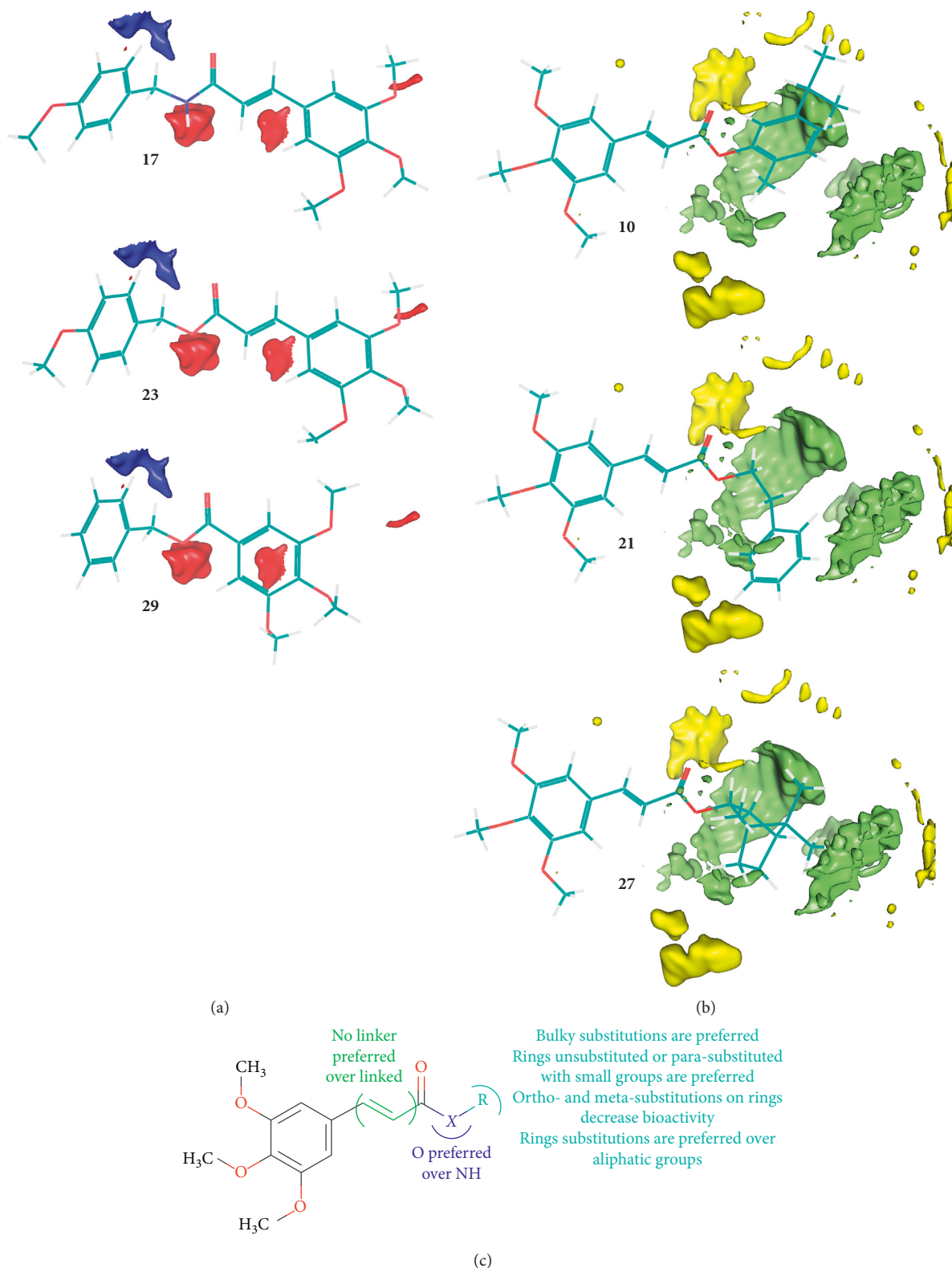


FIGURE 3: Summary of the 3D-QSAR model. (a) Influence of the electrostatic properties of the compounds on bioactivity. (b) Influence of the steric factor on bioactivity. (c) Summary of the SAR derived from the 3D-QSAR analyses.

(0.564  $\mu\text{M}$ ) for **1** and 145  $\mu\text{g/ml}$  (0.608  $\mu\text{M}$ ) for **2** [18, 19]. In addition, pipartine (**1**) was tested against promastigote forms of *L. infantum* and *L. amazonensis* and reached  $\text{IC}_{50}$

values of 7.9 and 3.3  $\mu\text{M}$ , respectively (positive control: amphotericin B,  $\text{IC}_{50} = 0.2 \mu\text{M}$ ). These results demonstrate the potential antileishmanial activity of pipartine and



3,4,5-trimethoxycinnamic acid, justifying the choice of these compounds as starting materials for the planning of new derivatives with higher antileishmanial activities [20].

**2.3. Structure-Activity Relationship (SAR).** The assayed compounds in this study were divided into three groups: analogues **5–21** (cinnamic esters), analogues **22–34** (amides), and analogues **35–36** (benzoic esters). Previous studies have investigated different compounds containing the 3,4,5-trimethoxyphenyl ring in order to understand its contribution to the biological activity [21]. For example, in a study performed by Dong-Jun et al., the authors showed that 3,4,5-trimethoxyphenyl moiety at the *N*-1 position of the  $\beta$ -lactam-azide derivatives was crucial for the antiproliferative activity against MGC-803, MCF-7, and A549 cancer cell lines [22]. Furthermore, anticancer compounds such as colchicine, steganacin, phenstatin, podophyllotoxin, combretastatin, and other synthetic analogues of these compounds share a 3,4,5-trimethoxyphenyl moiety as a common structural feature [23]. Thus, herein we preserved the (*E*)-3-(3,4,5-trimethoxyphenyl)-acryloyl moiety on cinnamic esters and amides and changed this moiety on benzoic esters (without the spacer group in the chemical structure).

Analysis on the structure-activity relationship revealed that, in general, an acrylate moiety on cinnamic esters appears to be more important for improving antileishmanial activity when compared to the acrylamide moiety on amides. This effect can be clearly observed comparing compounds **13** ( $IC_{50} = 0.101 \pm 0.031 \mu M$ ) and **29** ( $IC_{50} = 0.662 \pm 0.188 \mu M$ ), whose only difference is the replacement of the OH group **13** by NH **29** at this position, being compound **13** 6.6-fold more active than **29**.

The chemical structure of ester **36** ( $IC_{50} = 0.025 \pm 0.009 \mu M$ ) differs from other compounds by a molecular simplification of the (*E*)-3-(3,4,5-trimethoxyphenyl)-acryloyl moiety with removal of the ethylene group (carbons 2 and 3) and another simplification by changing from phenylethyl radical to benzyl. This structural modification contributed to increase the antileishmanial activity, since compound **36** ( $IC_{50} = 0.02 \pm 0.01 \mu M$ ) was more active than the ester **14** ( $IC_{50} = 0.975 \pm 0.241$ ). In addition, the comparison can also be made with amide **26** ( $IC_{50} = 0.734 \pm 0.252 \mu M$ ), a structural analogue containing the same benzyl radical attached to the (*E*)-3-(3,4,5-trimethoxyphenyl)-acrylamide moiety [12, 19, 24, 25]. Similarly, ester **36** showed more potent antileishmanial activity than amide **26**.

The ester **20** ( $IC_{50} = 0.007 \pm 0.008 \mu M$ ) containing the monoterpenic substructure bornyl attached on the (*E*)-3-(3,4,5-trimethoxyphenyl)-acryloyl moiety yielded the best  $IC_{50}$  value, near the positive control amphotericin B ( $IC_{50} = 0.0015 \mu M$ ). This result demonstrates the importance of this radical on antileishmanial activity and can be a prototype for the planning of new derivatives with higher antileishmanial activities. In an earlier study, a series of compounds based on caffeic acid bornyl ester was synthesized and tested *in vitro* against *L. major*, *L. donovani* promastigotes, and *L. major* amastigotes to investigate the SAR. The results showed that the bornyl moiety was

important for the antileishmanial activity. The most active compounds ( $IC_{50}$  values varying between 15.6 and 50.2  $\mu M$ ) were all esters of borneol, namely caffeic acid (–)-bornyl ester, caffeic acid isobornyl ester, cinnamic acid (–)-bornyl ester, and phenyl propanoic acid (–)-bornyl ester [1].

Esters **14** ( $IC_{50} = 0.975 \pm 0.241 \mu M$ ), **16** ( $IC_{50} = 0.513 \pm 0.065 \mu M$ ), and **19** ( $IC_{50} > 1.041 \mu M$ ), containing aromatic groups, decreased the antileishmanial activity when compared with some amides (**28**,  $IC_{50} = 0.109 \pm 0.010 \mu M$ ). However, the esters **17** ( $IC_{50} = 0.083 \pm 0.016 \mu M$ ) and **20** ( $IC_{50} = 0.007 \pm 0.008 \mu M$ ) gave better results, demonstrating that the biological effect of these changes is not easily predictable [9, 12]. The introduction of methyl groups contributes to increase lipophilicity. It was observed that the methyl group of the ester **15** ( $IC_{50} = 0.125 \pm 0.035 \mu M$ ) in the *para*-position on the phenylethyl moiety was the determinant change to improve the antileishmanial activity when compared with ester **14** ( $IC_{50} = 0.975 \pm 0.24 \mu M$ ) lacking this group [9, 12].

The introduction of methylene groups in general increases the lipophilicity, providing lower  $IC_{50}$  values. Table 1 shows that the antileishmanial activity of esters **5** ( $IC_{50} = 0.641 \pm 0.052 \mu M$ ), **6** ( $IC_{50} = 0.257 \pm 0.041 \mu M$ ), and **7** ( $IC_{50} = 0.09 \pm 0.032 \mu M$ ) was inversely proportional to the length of the carbon chain attached to (*E*)-3-(3,4,5-trimethoxyphenyl)-acrylate. For esters **9** ( $IC_{50} = 0.149 \pm 0.025 \mu M$ ) and **10** ( $IC_{50} = 0.133 \pm 0.014 \mu M$ ), the  $IC_{50}$  values have increased compared to **7**, demonstrating that from four carbons the antileishmanial activity begins to decrease, with exception of ester **11** ( $IC_{50} = 0.076 \pm 0.009 \mu M$ ) that even with decyl radical provided  $IC_{50}$  near the ester **7** ( $IC_{50} = 0.09 \pm 0.032 \mu M$ ) [12, 26].

Branches on side-chains *R* of esters **8** ( $IC_{50} = 0.194 \pm 0.04 \mu M$ ) and **17** ( $IC_{50} = 0.083 \pm 0.016 \mu M$ ) did not provide better results compared to esters of saturated chains. However, the aromatic rings of ester **17** were determinant to improve the antileishmanial activity when compared to ester **8**. The exchange of side-chain *R*, from butyl in ester **9** ( $IC_{50} = 0.149 \pm 0.025 \mu M$ ) to methoxyethyl in ester **12** ( $IC_{50} = 0.076 \pm 0.022 \mu M$ ), reduced the  $IC_{50}$  value. On ester **18** ( $IC_{50} = 0.029 \pm 0.007 \mu M$ ), the furfuryl radical reduced the molecular flexibility and, compared to ester **12**, improved the antileishmanial activity. A molecular simplification approach was tried on ester **35** ( $IC_{50} = 0.656 \pm 0.049 \mu M$ ) compared to ester **12**, but did not provide better results. However, the presence of oxygen on the methoxyethyl group on side-chain *R* of ester **36** ( $IC_{50} = 0.025 \pm 0.009 \mu M$ ) contributed to increase the antileishmanial activity [12, 24, 25].

The increase of stiffness on side-chain *R* of ester **21** ( $IC_{50} = 0.042 \pm 0.011 \mu M$ ), containing two atoms of oxygen of the dioxolane group fused on benzyl, increased the antileishmanial activity when compared to ester **13** ( $IC_{50} = 0.101 \pm 0.031 \mu M$ ) with 4-methoxybenzyl radical. Comparing the saturated side-chain *R* on amides **22** ( $IC_{50} = 0.577 \pm 0.080 \mu M$ ) and **24** ( $IC_{50} = 0.564 \pm 0.061 \mu M$ ) with the six-membered ring on amide **25** ( $IC_{50} = 0.117 \pm 0.027 \mu M$ ), it was observed that the replacement of saturated side-chains *R* by rigid groups increased the antileishmanial activity also on amides [12, 24, 25]. Compound **23**

( $IC_{50} = 0.091 \pm 0.015 \mu\text{g/ml}$ ) with a tertiary amide provides better result compared to **27** ( $IC_{50} = 0.353 \pm 0.080 \mu\text{M}$ ).

Replacing the methyl groups attached to the aromatic ring with the methoxy group dramatically decreased the antileishmanial activity in series of amide analogues, and this reduction was dependent on the number of substituted groups. For example, compound **28** ( $R_3 = \text{CH}_3$ ) exhibited an  $IC_{50}$  value of  $0.109 \pm 0.010 \mu\text{M}$ , whereas compounds **29** ( $R_3 = \text{OCH}_3$ ), **33** ( $R_1$  and  $R_3 = \text{OCH}_3$ ), and **34** ( $R_1$  and  $R_3 = \text{OCH}_3$ ) revealed  $IC_{50}$  values of  $0.662 \pm 0.188$ ,  $>1.033$  and  $>1.033$ , respectively. Similarly, the addition of halogens atoms (Br, F or Cl) to the aromatic ring of amide series also reduced the antileishmanial activity, since compounds **30** ( $R_3 = \text{Br}$ ,  $IC_{50} = 1.137 \pm 0.252 \mu\text{M}$ ), **31** ( $R_3 = \text{Br}$ ,  $IC_{50} > 1.108 \mu\text{M}$ ), and **32** ( $R_3 = \text{Br}$ ,  $IC_{50} = 0.486 \pm 0.043 \mu\text{M}$ ) showed weak or no activity.

### 3. Experimental

**3.1. Chemical Characterization and Reagents.** The  $^1\text{H}$  and  $^{13}\text{C}$  NMR and IR spectral data were recorded, and their signals were compared with published data. For compounds **18**, **19**, **21**, **32**, **33**, **34**, and **35**, the spectrometric methods LS-MALDI TOF/TOF or ESI-TOF were used to confirm the chemical structures. The preparation and structural characterization data of compounds **5–9**, **10–12**, **14–17**, **22**, **23**, **26**, **28**, **29**, and **31** were published in a previous article [21].

All used reagents were of reagent grade and purchased from Sigma Aldrich. The following equipments were used: Irprestige-21 Shimadzu Fourier Transform spectrophotometer (Shimadzu, Kyoto, Japan) for IR, and Varian Mercury spectrometer (Palo Alto, CA, USA) 200 MHz for  $^1\text{H}$  NMR and 50 MHz for  $^{13}\text{C}$  NMR. The standard for chemical shifts was the  $\text{CDCl}_3$  or TMS solvent peak. For HR-MS, the LS-MALDI TOF/TOF apparatus was used equipped with a high-performance laser ( $\lambda = 355 \text{ nm}$ ) and a reflector operated by the software FlexControl 2.4 (Bruker Daltonics G, bsH, Bremen, Germany), and microOTOF operated by software Bruker Compass DataAnalysis 4.0 (Bruker Daltonics G, bsH, Bremen, Germany). Melting points were measured on an equipment Tecnal PFM-II, 220 V. To measure the optical activity of **20** and of starting material (–)-borneol a digital polarimeter P-2000 (Jasco) was used after standardization with 98% anhydrous methanol.

**3.2. General Procedure for Preparation of Compound 35.** To a solution of 0.25 g of carboxylic acid in 250 ml of ROH under stirring, 0.5 ml of 96% (v/v)  $\text{H}_2\text{SO}_4$  were added and solution was refluxed for 3 h. After removing of half ROH under reduced pressure, the solution was diluted in 10 ml of water, and product was extracted with ethyl acetate. Then, the product was successively washed with 5% (w/v)  $\text{NaHCO}_3$  and water and dried with anhydrous  $\text{Na}_2\text{SO}_4$ . Finally, the solvent was evaporated to yield the pure compound [27–29].

**3.3. 2-Methoxyethyl 3,4,5-trimethoxybenzoate (35).** Yield 91%; brown solid; MM: 270.11 g/mol; m.p.: 32–35°C;  $^1\text{H}$  NMR (200 MHz,  $\text{CDCl}_3$ ):  $\delta_{\text{H}}$  7.31 (s, 2H), 4.51–4.40 (m, 2H),

3.89 (s, 9H), 3.77–3.66 (m, 2H), 3.40 (s, 3H);  $^{13}\text{C}$  NMR (50 MHz,  $\text{CDCl}_3$ ):  $\delta_{\text{C}}$  166.0, 152.7, 142.1, 124.9, 106.8, 70.4, 64.0, 60.7, 58.8, 56.0; IR  $\nu_{\text{max}}$  (KBr,  $\text{cm}^{-1}$ ): 2941, 2839, 1715, 1589, 1504, 864; microOTOF:  $m/z$  [ $\text{M} + \text{Na}$ ] $^+$  293.3107 (calcd. for  $\text{C}_{13}\text{H}_{18}\text{O}_6$ : 293.1103).

**3.4. General Procedure for Preparation of Compound 13.** In a 50 ml round-bottom flask, 0.42 mmol (0.1 g) of 3,4,5-trimethoxycinnamic acid were dissolved in 5.0 ml of acetone. Then, 1.68 mmol (0.22 ml) of  $\text{Et}_3\text{N}$  and 0.43 mmol of alkyl halide were added in the same solution, and the reaction mixture was refluxed for 48 h. The acetone was removed under reduced pressure, and the content of the reactions was diluted in 10 ml of ethyl acetate and 10 ml of water. The products were extracted thrice with 10 ml of ethyl acetate. Afterwards, organic phases were successively washed with 5% (w/v)  $\text{NaHCO}_3$  and water, dried over anhydrous  $\text{Na}_2\text{SO}_4$ , and filtered. The product was purified via a silica gel 60 column chromatography (mobile phase: hexane-ethyl acetate (1 : 1)) [30].

**3.4.1. (E)-4-Methoxybenzyl 3-(3,4,5-trimethoxyphenyl)acrylate (13).** Yield 77.4%; white solid; MM: 358.14 g/mol; m.p.: 110–111°C;  $^1\text{H}$  NMR (200 MHz,  $\text{CDCl}_3$ ):  $\delta_{\text{H}}$  7.61 (d,  $J = 16 \text{ Hz}$ , 1H), 7.34 (d,  $J = 2.0 \text{ Hz}$ , 2H), 6.90 (d,  $J = 2.0 \text{ Hz}$ , 2H), 6.73 (s, 2H), 6.37 (d,  $J = 16 \text{ Hz}$ , 1H), 5.17 (s, 2H), 3.85 (s, 9H), 3.80 (s, 3H);  $^{13}\text{C}$  NMR (50 MHz,  $\text{CDCl}_3$ ):  $\delta_{\text{C}}$  166.8; 159.7; 153.5; 145.0; 140.2; 130.2; 129.9; 128.2; 117.3; 114.0; 105.3; 66.3; 61.0; 56.2; 55.3; IR  $\nu_{\text{max}}$  (KBr,  $\text{cm}^{-1}$ ): 2999, 2939, 2837, 1709, 1636, 1034, 1005, 1584, 1506, 825, 609; LS-MALDI TOF/TOF  $m/z$  [ $\text{M}$ ] $^+$  358.1353 (calcd. for  $\text{C}_{20}\text{H}_{22}\text{O}_6$ : 358.1416).

**3.5. General Procedure for Preparation of Compounds 18–21.** To a solution of 0.1 g (0.42 mmol) of 3,4,5-trimethoxycinnamic acid dissolved in 6.3 ml of  $\text{CH}_2\text{Cl}_2$ , 0.54 mmol of ROH and 0.015 g of DMAP were added. After 5 min of stirring, 0.1 g (0.54 mmol) of DCC was also added. Stirring was continued overnight at room temperature. The solvent was removed under vacuum, and the remaining content was diluted in 10 ml of ethyl acetate and 10 ml of water. The product was extracted with 10 ml ethyl acetate (three times), and the organic phases were successively washed with 5% (w/v)  $\text{NaHCO}_3$  and water, dried over anhydrous  $\text{Na}_2\text{SO}_4$ , and filtered. After removing ethyl acetate under vacuum, the products were purified on a silica gel 60 column chromatography (mobile phase: hexane-ethyl acetate).

**3.5.1. (E)-Furfuryl 3-(3,4,5-trimethoxyphenyl)acrylate (18).** Yield 79%; brown oil; MM: 318.11 g/mol;  $^1\text{H}$  NMR (200 MHz,  $\text{CDCl}_3$ ):  $\delta_{\text{H}}$  7.58 (d,  $J = 16.0 \text{ Hz}$ , 1H), 7.43–7.37 (m, 1H), 6.69 (s, 2H), 6.45–6.16 (m, 3H), 5.15 (s, 2H), 3.81 (s, 6H), 3.83 (s, 3H);  $^{13}\text{C}$  NMR (50 MHz,  $\text{CDCl}_3$ ):  $\delta_{\text{C}}$  166.4, 153.3, 149.5, 145.3, 143.3, 140.0, 129.7, 116.7, 110.7, 110.6, 105.5, 60.8, 58.0, 56.0; IR  $\nu_{\text{max}}$  (KBr,  $\text{cm}^{-1}$ ): 2997, 2939, 2839, 1713, 1634, 1003, 1582, 1504, 827; LS-MALDI TOF/TOF  $m/z$  [ $\text{M}$ ] $^+$  318.1103 (calcd. for  $\text{C}_{17}\text{H}_{18}\text{O}_6$ : 318.1103).

3.5.2. (*E*)-Eugenyl 3-(3,4,5-trimethoxyphenyl)-acrylate (**19**). Yield 86%; white solid; MM: 384.16 g/mol; m.p.: 170–172°C; <sup>1</sup>H NMR (200 MHz, CDCl<sub>3</sub>): δ<sub>H</sub> 7.77 (d, *J* = 16.0 Hz, 1H), 7.00 (d, 1H, *J* = 6.0 Hz), 6.83–6.73 (m, 4H), 6.58 (d, *J* = 16.0 Hz, 1H), 6.08–5.83 (m, 1H), 5.18–5.02 (m, 2H), 3.88 (s, 3H), 3.86 (s, 6H), 3.80 (s, 3H), 3.37 (d, *J* = 6.0 Hz, 2H); <sup>13</sup>C NMR (50 MHz, CDCl<sub>3</sub>): δ<sub>C</sub> 165.0, 153.4, 151.0, 146.4, 140.2, 139.0, 137.9, 137.0, 129.7, 122.6, 120.6, 116.3, 116.1, 112.7, 105.3, 60.9, 56.0, 55.8, 40.1; IR ν<sub>max</sub> (KBr, cm<sup>-1</sup>): 3067, 2968, 2939, 2839, 1722, 1630, 1034, 1009, 1582, 1508, 824; LS-MALDI TOF/TOF *m/z* [M]<sup>+</sup> 384.1575 (calcd. for C<sub>22</sub>H<sub>24</sub>O<sub>6</sub>: 384.1573).

3.5.3. (*E*)-(-)-Bornyl 3-(3,4,5-trimethoxyphenyl)-acrylate (**20**). Yield 87%; white solid; MM: 374.21 g/mol; m.p.: 100–102°C; <sup>1</sup>H NMR (200 MHz, CDCl<sub>3</sub>): δ<sub>H</sub> 7.54 (d, *J* = 16.0 Hz, 1H), 6.73 (s, 2H), 6.34 (d, *J* = 16.0 Hz, 1H), 4.98 (d, *J* = 8.0 Hz, 1H), 3.85 (s, 9H), 2.47–2.28 (m, 1H), 2.05–1.96 (m, 1H), 1.67 (d, *J* = 4.0 Hz, 1H), 1.37–1.15 (m, 3H), 1.07–0.95 (m, 1H), 0.90 (s, 3H), 0.84 (s, 6H); <sup>13</sup>C NMR (50 MHz, CDCl<sub>3</sub>): δ<sub>C</sub> 167.2, 153.4, 144.2, 139.9, 130.0, 118.0, 105.1, 79.9, 60.9, 56.1, 48.9, 47.9, 44.9, 36.9, 28.1, 27.3, 19.7, 18.9, 13.6; IR ν<sub>max</sub> (KBr, cm<sup>-1</sup>): 2953, 2839, 1697, 1634, 1026, 1007, 1582, 1504, 831; [α]<sub>D</sub><sup>25°C</sup> = -5.5° (c 0.001, MeOH), RSD: 4.3% [31].

3.5.4. (*E*)-Piperonyl-3-(3,4,5-trimethoxyphenyl)-acrylate (**21**). Yield 30%; white solid; MM: 372.12 g/mol; m.p.: 123–126°C; <sup>1</sup>H NMR (200 MHz, CDCl<sub>3</sub>): δ<sub>H</sub> 7.61 (d, *J* = 16.0 Hz, 1H), 6.93–6.76 (m, 3H), 6.74 (s, 2H), 6.36 (d, *J* = 16.0 Hz, 1H), 5.95 (s, 2H), 5.12 (s, 2H), 3.86 (s, 9H); <sup>13</sup>C NMR (50 MHz, CDCl<sub>3</sub>): δ<sub>C</sub> 166.8, 153.4, 147.9, 147.7, 145.1, 140.1, 129.9, 129.8, 122.4, 117.2, 109.1, 108.3, 105.2, 101.2, 66.4, 61.0, 56.2; IR ν<sub>max</sub> (KBr, cm<sup>-1</sup>): 3067, 2926, 2849, 1703, 1630, 1038, 1005, 1582, 1502, 854; LS-MALDI TOF/TOF *m/z* [M + H]<sup>+</sup> 373.1288 (calcd. for C<sub>20</sub>H<sub>20</sub>O<sub>7</sub> + H: 373.1268).

3.6. General Procedure for Preparation of Amides. To a solution of 0.1 g of 3,4,5-trimethoxycinnamic in 0.84 ml of DMF in a round-bottom flask, 0.06 ml (0.42 mmol) of trimethylamine was added. The solution was cooled in an ice water bath and 0.42 mmol of amine were added, followed by a solution of 0.42 mmol of BOP (0.84 ml) in CH<sub>2</sub>Cl<sub>2</sub>. After stirring for 30 min, the reaction continued at room temperature for 3 h. CH<sub>2</sub>Cl<sub>2</sub> was removed under vacuum, and the remaining solution was diluted in 10 ml of ethyl acetate and 10 ml of water. The product was extracted with 10 ml of ethyl acetate (three times), and the organic phases were washed successively with 1 N HCl, water, 1 M NaHCO<sub>3</sub>, and water, dried over anhydrous Na<sub>2</sub>SO<sub>4</sub>, filtered, and evaporated. The product was purified on a silica gel 60 column chromatography (mobile phase: hexane-ethyl acetate (1 : 1)).

3.6.1. (*E*)-*N*-Octyl-3-(3,4,5-trimethoxyphenyl)-acrylamide (**24**). Yield 62.4%; white solid; MM: 349.23 g/mol; m.p.: 133–134°C; <sup>1</sup>H NMR (200 MHz, CDCl<sub>3</sub>): δ<sub>H</sub> 7.50 (d, *J* = 16.0 Hz, 1H), 6.69 (s, 2H), 6.33 (d, *J* = 16.0 Hz, 1H), 6.00

(s, 1H), 3.83 (s, 9H), 3.34 (q, *J* = 6.0 Hz, 2H), 1.62–1.44 (m, 2H), 1.31–1.22 (m, 10H), 0.84 (t, *J* = 6.0 Hz, 3H); <sup>13</sup>C NMR (50 MHz, CDCl<sub>3</sub>): δ<sub>C</sub> 166.0, 153.4, 147.6, 140.7, 139.5, 130.6, 120.3, 104.7, 61.0, 56.1, 39.9, 31.9, 29.7, 29.4, 27.1, 22.7, 14.2; IR ν<sub>max</sub> (KBr, cm<sup>-1</sup>): 3290, 3003, 2955, 2924, 2853, 1655, 1622, 1580, 1504, 827 [32].

3.6.2. (*E*)-*N*-Cyclohexyl-3-(3,4,5-trimethoxyphenyl)-acrylamide (**25**). Yield 59%; white solid; MM: 319.18 g/mol; m.p.: 320–321°C; <sup>1</sup>H NMR (200 MHz, CDCl<sub>3</sub>): δ<sub>H</sub> 7.49 (d, *J* = 16.0 Hz, 1H), 6.68 (s, 2H), 6.34 (d, *J* = 16.0 Hz, 1H), 5.90 (s, 1H), 3.83 (s, 3H), 3.81 (s, 6H), 2.01–1.05 (m, 11H); <sup>13</sup>C NMR (50 MHz, CDCl<sub>3</sub>): δ<sub>C</sub> 165.0, 153.4, 140.5, 139.3, 130.6, 120.7, 104.8, 61.0, 56.1, 48.4, 33.3, 25.6, 24.9; IR ν<sub>max</sub> (KBr, cm<sup>-1</sup>): 3287, 3003, 2928, 2853, 1663, 1612, 1582, 1508, 822 [33].

3.6.3. (*E*)-1-(Pyrrolidine-1-yl)-3-(3,4,5-trimethoxyphenyl)-prop-2-en-1-one (**27**). Yield 72%; white solid; MM: 291.15 g/mol; m.p.: 233–235°C; <sup>1</sup>H NMR (200 MHz, CDCl<sub>3</sub>): δ<sub>H</sub> 7.59 (d, *J* = 16.0 Hz, 1H), 6.72 (s, 2H), 6.59 (d, *J* = 16.0 Hz, 1H), 3.86 (s, 6H), 3.84 (s, 3H), 3.68–3.51 (m, 4H), 2.07–1.79 (m, 4H); <sup>13</sup>C NMR (50 MHz, CDCl<sub>3</sub>): δ<sub>C</sub> 164.8, 153.4, 142.0, 139.5, 131.0, 118.0, 105.1, 61.0, 56.2, 46.8, 46.2, 26.2, 24.4; IR ν<sub>max</sub> (KBr, cm<sup>-1</sup>): 3049, 2963, 2939, 2839, 1645, 1605, 1580, 1504, 820 [29].

3.6.4. (*E*)-*N*-(4-Fluorobenzyl)-3-(3,4,5-trimethoxyphenyl)-acrylamide (**30**). Yield 87%; white solid; MM: 345.14 g/mol; m.p.: 195–196°C; <sup>1</sup>H NMR (200 MHz, CDCl<sub>3</sub>): δ<sub>H</sub> 7.57 (d, *J* = 16.0 Hz, 1H), 7.30–7.19 (m, 2H), 6.99 (t, *J* = 8.0 Hz, 2H), 6.69 (s, 2H), 6.39 (d, *J* = 14.0 Hz, 1H), 4.50 (d, *J* = 6.0 Hz, 2H), 3.85 (s, 3H), 3.82 (s, 6H); <sup>13</sup>C NMR (50 MHz, CDCl<sub>3</sub>): δ<sub>C</sub> 166.0, 164.7, 159.8, 153.4, 141.5, 139.6, 134.1, 130.4, 129.6, 129.5, 119.8, 115.8, 115.4, 105.0, 61.0, 56.1, 43.2; IR ν<sub>max</sub> (KBr, cm<sup>-1</sup>): 3291, 3012, 2959, 2932, 2839, 1651, 1616, 1580, 1508, 829 [34].

3.6.5. (*E*)-*N*-(4-Bromobenzyl)-3-(3,4,5-trimethoxyphenyl)-acrylamide (**32**). Yield 99.8%; white solid; MM: 405.6 g/mol; m.p.: 360–363°C; <sup>1</sup>H NMR (200 MHz, CDCl<sub>3</sub>): δ<sub>H</sub> 7.57 (d, *J* = 16.0 Hz, 1H), 7.43 (d, *J* = 8.00 Hz, 2H), 7.17 (d, *J* = 8.00 Hz, 2H), 6.70 (s, 2H), 6.45–6.15 (m, 2H), 4.49 (d, *J* = 6.0 Hz, 2H), 3.86 (s, 3H), 3.84 (s, 6H); <sup>13</sup>C NMR (50 MHz, CDCl<sub>3</sub>): δ<sub>C</sub> 166.0, 153.4, 141.6, 139.7, 137.4, 131.8, 13.4, 129.5, 121.4, 119.7, 105.0, 61.0, 56.2, 43.2; IR ν<sub>max</sub> (KBr, cm<sup>-1</sup>): 3292, 3044, 2957, 2932, 2835, 1651, 1614, 1582, 1506, 824; LS-MALDI TOF/TOF *m/z* [M]<sup>+</sup> 405.0558 (calcd. for C<sub>19</sub>H<sub>20</sub>BrNO<sub>4</sub>: 405.0576).

3.6.6. (*E*)-*N*-(2,4-Dimethoxybenzyl)-3-(3,4,5-trimethoxyphenyl)-acrylamide (**33**). Yield 23%; white solid; MM: 387.17 g/mol; m.p.: 235–238°C; <sup>1</sup>H NMR (200 MHz, CDCl<sub>3</sub>): δ<sub>H</sub> 7.50 (d, *J* = 16.0 Hz, 1H), 7.20 (d, *J* = 8.0 Hz, 1H), 6.67 (s, 2H), 6.42 (s, 1H), 6.41–6.23 (m, 3H), 4.46 (d, *J* = 6.0 Hz, 2H), 3.83 (s, 3H), 3.82 (s, 6H), 3.80 (s, 3H), 3.76 (s, 3H); <sup>13</sup>C NMR



(50 MHz, CDCl<sub>3</sub>):  $\delta_C$  165.6, 160.6, 158.6, 153.4, 140.8, 139.4, 130.6, 130.6, 120.4, 118.8, 104.9, 104.0, 98.6, 61.0, 56.1, 55.4, 39.1; IR  $\nu_{max}$  (KBr, cm<sup>-1</sup>): 3283, 3040, 3001, 2932, 2837, 1651, 1605, 1585, 1506, 820; LS-MALDI TOF/TOF  $m/z$  [M]<sup>+</sup> 387.1674 (calcd. for C<sub>21</sub>H<sub>25</sub>NO<sub>6</sub>: 387.1682).

3.6.7. (*E*)-*N*-(3,4-Dimethoxybenzyl)-3-(3,4,5-trimethoxyphenyl)-acrylamide (**34**). Yield 75%; white solid; MM: 387.17 g/mol; m.p.: 170–173°C; <sup>1</sup>H NMR (200 MHz, CDCl<sub>3</sub>):  $\delta_H$  7.48 (*d*, *J* = 16.0 Hz, 1H); 6.80–6.64 (*m*, 3H); 6.61 (*s*, 2H), 6.41 (*d*, *J* = 16.0 Hz, 1H), 4.38 (*d*, *J* = 6.0 Hz, 2H), 3.76 (*s*, 3H), 3.73 (*s*, 3H), 3.71 (*s*, 9H); <sup>13</sup>C NMR (50 MHz, CDCl<sub>3</sub>):  $\delta_C$  165.9, 153.2, 148.9, 148.2, 140.8, 139.3, 130.7, 130.3, 120.1, 120.0, 111.0, 104.8, 60.8, 55.9, 43.5; IR  $\nu_{max}$  (KBr, cm<sup>-1</sup>): 3370, 3061, 2961, 2926, 2853, 1670, 1585, 1502, 827; LS-MALDI TOF/TOF  $m/z$  [M + Na]<sup>+</sup> 410.1579 (calcd. for C<sub>21</sub>H<sub>25</sub>NO<sub>6</sub> + Na: 410.1580).

### 3.7. General Procedure for Preparation of Compound 36.

To a 5 ml round-bottom flask with 0.1 g (0.47 mmol) of 3',4',5'-trimethoxyacetophenone in 0.1 ml (0.94 mmol) of benzylic alcohol, the solution of 0.007 g of CuBr (0.047 mmol) in 0.07 ml (0.94 mmol) of pyridine was added, and then the solution of 0.025 mmol BF<sub>3</sub>·Et<sub>2</sub>O in 0.5 ml of chlorobenzene was added dropwise. The mixture was then stirred at 130°C open air for 10 h. After cooling at room temperature, chlorobenzene was removed under reduced pressure. The remaining content was diluted in 10 ml of ethyl acetate and 10 ml of water. The product was extracted with 10 ml of ethyl acetate (three times), and the organic phase was successively washed with 5% (w/v) NaHCO<sub>3</sub> and water, dried over anhydrous Na<sub>2</sub>SO<sub>4</sub>, and filtered. After the removal of ethyl acetate under vacuum, the product was purified on a silica gel 60-column chromatography (mobile phase: hexane-ethyl acetate) [35].

3.7.1. Benzyl 3,4,5-trimethoxybenzoate (**36**). Yield 56%; yellow oil; MM: 307.12 g/mol; <sup>1</sup>H NMR (200 MHz, CDCl<sub>3</sub>):  $\delta_H$  7.37–7.27 (*m*, 5H), 7.25 (*s*, 2H), 5.28 (*s*, 2H), 3.81 (*m*, 6H), 3.80 (*s*, 3H); <sup>13</sup>C NMR (50 MHz, CDCl<sub>3</sub>):  $\delta_C$  166.1, 153.0, 142.3, 136.1, 128.7, 128.3, 128.2, 125.2, 107.0, 66.9, 61.0, 56.3; IR  $\nu_{max}$  (KBr, cm<sup>-1</sup>): 2999, 2939, 2837, 1713, 1589, 1502, 864 [36].

3.8. *Leishmania Culture Conditions*. *Leishmania amazonensis* promastigote forms (IFLA/BR/67/PH8) were cultivated at 26°C in Schneider's medium (Sigma) supplemented with 10% fetal bovine serum (FBS) (Gibco BRL, Gaithersburg, MD, USA) and the antibiotic gentamicin (40 µg/ml) (Schering-Plough, Rio de Janeiro, Brazil).

3.9. *MTT Assay*. The antileishmanial activity on promastigote forms of *L. amazonensis* was evaluated using the MTT (3-(4,5-dimethylthiazol-2-yl)-2,5-diphenyltetrazolium bromide) method (Amaresco, Ohio, USA). The promastigotes of *L. amazonensis* were distributed in a 96-well plate

(1 × 10<sup>6</sup> cells) and treated with different concentrations of piplartine derivatives (**5–36**) (400, 200, 100, 50, 25, 12.5, 6.25, and 3.125 µg/ml) diluted in Schneider's medium (Sigma) supplemented with 10% FBS. The plates were incubated for 72 hours at 34°C. After the incubation period, 10 µl of a 5 mg/ml MTT solution in PBS was added to each well. After treatment, the plate was incubated for additional 4 hours, and at the end 50 µl of a solution of 10% sodium dodecyl sulphate (Sigma Chemical-st. Louis, MO, USA) was added and left overnight to allow dissolution of the crystals of formazan [37]. Finally, the absorbance reading was performed using a spectrophotometer (Biotek model Elx800) at 540 nm. The Schneider medium was used as negative control, and amphotericin B, a reference drug for treatment of visceral leishmaniasis, was used as positive control [37]. The IC<sub>50</sub> values were defined as the concentration of each compound that reduced the absorbance of treated cells by 50% when compared with the cell control. All assays were performed in triplicate.

3.10. *Alamar Blue Assay*. To assess the cytotoxicity against normal cells, the cell line MRC-5 (human lung fibroblast) was obtained from the American Type Culture Collection (ATCC, Manassas, VA, USA) and was cultured as recommended by the ATCC. The cell culture was tested for mycoplasma using Mycoplasma Stain Kit (Sigma-Aldrich) to validate the use of cells free from contamination. The cell viability was measured colorimetrically using the alamarBlue assay [38]. Shortly, compounds **18**, **20**, and **36** (dissolved in DMSO and diluted in the RPMI-1640 medium at a range of eight different concentrations from 0.19 to 25 µg/ml) were added to each well and incubated for 72 h. Doxorubicin (Sigma-Aldrich) was used as the positive control. Four hours before the end of incubation, 20 µl of a stock solution (0.312 mg/ml) of resazurin (Sigma-Aldrich) was added to each well. Absorbance was measured at 570 nm and 600 nm using the SpectraMax 190 Microplate Reader (Molecular Devices, Sunnyvale, CA, USA). The half maximal inhibitory concentration (IC<sub>50</sub>) values with 95% confidence intervals were obtained by nonlinear regression using GraphPad Prism (Intuitive Software for Science; San Diego, CA, USA).

## 4. Methods

The first step for modeling was obtaining the initial 3D structure of each compound using the OpenEye's Omega software [39]. Fragments for 3D structures generation were obtained with MAKEFRAGLIB, which is a part of the OMEGA suite. The Merck Molecular Force Field (MMFF94s) excluding the Coulomb interactions (mmff94s\_NoEstat) was employed for fragment generation. Fragments with 4.0 kcal above the global minimum as well as those with a RMS distance lower than 0.1 from any conformer in the database were discarded. Default parameters were used for generating one 3D conformation per compound with OMEGA. Conformational exploration and alignment of the compounds were performed with the Open3DALIGN software [40]. A conformational library of each compound was obtained

through quenched molecular dynamics (QMD) conformational searches that employed TINKER with an implicit solvent model [41]. Two hundred molecular dynamic simulations of length 100 ps were performed for each compound. The remaining parameters for the QMD in Open3DALIGN were kept to their default values. Structural alignment took place was performed using a method that combines atom- and pharmacophore-based alignments as implemented in Open3DALIGN.

3D-QSAR models were developed with the Open3DQSAR suite [42], which performs partial least squares (PLS) regression models from molecular interaction fields (MIF). Unless otherwise noted, default parameters were employed for Open3DQSAR. The input to Open3DQSAR is a set of aligned conformers of the dataset with associated bioactivities. The best alignment produced by Open3DALIGN in the previous step was used for 3D-QSAR models generation. In this study, compounds 19, 26, 31, and 32 were removed from the modeling process because of their undetermined  $IC_{50}$ . The bioactivity of the remaining compounds was transformed to  $pIC_{50}$  values ( $pIC_{50} = -\log_{10} IC_{50}$ ), provided that  $IC_{50}$  values are expressed in molar units.

A grid was constructed around the aligned molecules in such a way that its box exceeded in 5 Å the largest molecule and grid spacing was set to 0.5 Å. Steric and electrostatic molecular mechanics of MIFs were computed using the Merck force field (MMFF94). For the computation of both MIFs, an alkyl carbon (charge +1) was used as probe. Before model construction, variables were filtered to discard those with van der Waals energies above  $10^4$  kcal/mol. Corresponding points on the electrostatic MIF were also removed. For both MIFs, energies greater than 30 kcal/mol or lower than -30 kcal/mol were set to 30 kcal/mol and -30 kcal/mol, respectively. Also values of energy between -0.05 and 0.05 kcal/mol were set to 0 in the two MIFs, and all variables with standard deviation lower than 0.1 were discarded. All variables spanning up to four levels were removed from both fields. As a final filter, variables were scaled employing the AUTO option of Open3DQSAR.

Initial PLS models considered 10 principal components. The optimal number of principal components (PCs) was selected based on the value of the Leave One Out cross-validation  $R^2$  ( $q^2$ ). Variables were then grouped using the Smart Region definition procedure implemented in Open3DQSAR taking into account the previously identified optimal number of PCs. The grouped variables were subject to a selection procedure according to the Fractional Factorial Design using Leave Many Out (LMO) cross validation with 20 runs and 5 groups. Only selected variables in previous step were kept on the dataset. After these variable selection procedures, the PLS model was recomputed considering the optimal number of PCs and validated using the LOO and LMO strategies.

## 5. Conclusion

We synthesized a series of 32 pipartine analogues. The preliminary bioassay revealed that the most prominent compounds had rigid rings as substituents. Compound 18

contains a furfuryl portion attached to the (*E*)-3-(3,4,5-trimethoxyphenyl)-acryloyl moiety. This modification significantly improved the bioactivity. Molecular simplification of 36 in relation to other derivatives formed an analogue with better biological activity against *Leishmania*. Furthermore, bornyl radical appears to be important for the bioactivity, given that compound 20 revealed the strongest antileishmanial activity. Together, these results show that compounds 18, 20, and 36 are promising lead compounds in the development of new options of pharmacotherapeutic drugs for leishmaniasis.

## Data Availability

The data used to support the findings of this study are available from the corresponding author upon request.

## Conflicts of Interest

The authors declare that they have no conflicts of interest.

## Acknowledgments

This work was supported by the Brazilian agencies Conselho Nacional de Desenvolvimento Científico e Tecnológico (CNPq) and Coordenação de Aperfeiçoamento de Pessoal de Nível Superior (CAPES).

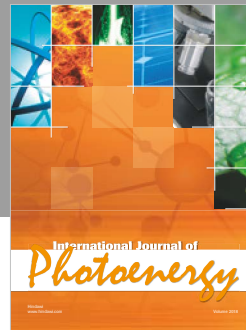
## References

- [1] J. Glaser, M. Schultheis, S. Hazra et al., "Antileishmanial lead structures from nature: analysis of structure-activity relationships of a compound library derived from caffeic acid bornyl ester," *Molecules*, vol. 19, no. 2, pp. 1394–1410, 2014.
- [2] L. C. L. R. Santana, S. M. P. Carneiro, L. B. Caland-Neto et al., "Brazilian brown propolis elicits antileishmanial effect against promastigote and amastigote forms of *Leishmania amazonensis*," *Natural Product Research*, vol. 28, no. 5, pp. 340–343, 2013.
- [3] D. N. Dortmund, "Early detection of comorbidity in psoriasis: recommendations of the national conference on healthcare in psoriasis," *Journal der Deutschen Dermatologischen Gesellschaft*, vol. 13, no. 7, pp. 191–201, 2015.
- [4] S. Tagboto and S. Townson, "Antiparasitic properties of medicinal plants and other naturally occurring products," *Advances in Parasitology*, vol. 50, pp. 199–295, 2001.
- [5] D. Ndjonka, L. Rapado, A. Silber, E. Liebau, and C. Wrenger, "Natural products as a source for treating neglected parasitic diseases," *International Journal of Molecular Sciences*, vol. 14, no. 2, pp. 3395–3439, 2013.
- [6] S. Sundar and J. Chakravarty, "An update on pharmacotherapy for leishmaniasis," *Expert Opinion on Pharmacotherapy*, vol. 16, no. 2, pp. 237–252, 2014.
- [7] H. S. Bodiwala, G. Singh, R. Singh et al., "Antileishmanial amides and lignans from *Piper cubeba* and *Piper retrofractum*," *Journal of Natural Medicines*, vol. 61, no. 4, pp. 418–421, 2007.
- [8] D. P. Bezerra, G. C. G. Militão, F. O. de Castro et al., "Piplartine induces inhibition of leukemia cell proliferation triggering both apoptosis and necrosis pathways," *Toxicology in Vitro*, vol. 21, no. 1, pp. 1–8, 2007.

- [9] E. J. Barreiro, A. E. Kümmerle, and C. A. M. Fraga, "The methylation effect in medicinal chemistry," *Chemical Reviews*, vol. 111, no. 9, pp. 5215–5246, 2011.
- [10] G. Müller, M. Albers, R. Fischer et al., "Discovery and evaluation of piperidinyl carboxylic acid derivatives as potent  $\alpha 4\beta 1$  integrin antagonists," *Bioorganic and Medicinal Chemistry Letters*, vol. 11, no. 23, pp. 3019–3021, 2001.
- [11] M. Hernandez, S. M. Cavalcanti, D. R. Moreira, W. de Azevedo Junior, A. C. Leite, and A. C. L. Leite, "Halogen atoms in the modern medicinal chemistry: hints for the drug design," *Current Drug Targets*, vol. 11, no. 3, pp. 303–314, 2010.
- [12] G. Thomas, *Medicinal Chemistry an Introduction*, Vol. 1, John Wiley & Sons, London, UK, 2nd edition, 2009.
- [13] T. T. Vogt, "Phenylpropanoid biosynthesis," *Molecular Plant*, vol. 3, no. 1, pp. 2–20, 2010.
- [14] J. Han, L. Li, L. Han, X. Huang, and T. Yuan, "Phenylpropanoid amides and phenylethanols from nanophyton erinaceum," *Biochemical Systematics and Ecology*, vol. 61, pp. 399–401, 2015.
- [15] J. Sun, Y.-L. Song, J. Zhang et al., "Characterization and quantitative analysis of phenylpropanoid amides in eggplant (*Solanum melongena* L.) by high performance liquid chromatography coupled with diode array detection and hybrid ion trap time-of-flight mass spectrometry," *Journal of Agricultural and Food Chemistry*, vol. 63, no. 13, pp. 3426–3436, 2015.
- [16] J. Glaser, M. Schultheis, H. Moll, B. Hazra, and U. Holzgrabe, "Antileishmanial and cytotoxic compounds from valeriana wallichii and identification of a novel nepetolactone derivative," *Molecules*, vol. 20, no. 4, pp. 5740–5753, 2015.
- [17] W. M. Abdel-Mageed, E. Y. Backheet, A. A. Khalifa, Z. Z. Ibraheim, and S. A. Ross, "Antiparasitic antioxidant phenylpropanoids and iridoid glycosides from *Tecoma mollis*," *Fitoterapia*, vol. 83, no. 3, pp. 500–507, 2012.
- [18] M. G. P. R. Ferreira, A. M. Kayano, I. Silva-Jardim et al., "Antileishmanial activity of 3-(3,4,5-trimethoxyphenyl) propanoic acid purified from amazonian piper tuberculatum Jacq., Piperaceae, fruits," *Revista Brasileira de Farmacognosia*, vol. 20, no. 6, pp. 1003–1006, 2010.
- [19] K. M. D. Araújo-Vilges, S. V. D. Oliveira, S. C. P. Couto et al., "Effect of pipartine and cinnamides on leishmania amazonensis, plasmodium falciparum and on peritoneal cells of Swiss mice," *Pharmaceutical Biology*, vol. 55, no. 1, pp. 1601–1607, 2017.
- [20] F. L. Moreira, T. B. Riul, M. L. Moreira et al., "Leishmanicidal effects of piperlongumine (pipartine) and its putative metabolites," *Planta Medica*, vol. 84, no. 15, pp. 1141–1148, 2018.
- [21] F. R. Da Nóbrega, O. Ozdemir, S. C. S. Nascimento Sousa, J. N. Barboza, H. Turkez, and D. P. De Sousa, "Piplartine analogues and cytotoxic evaluation against glioblastoma," *Molecules*, vol. 23, no. 6, p. 1382, 2018.
- [22] D. J. Fu, L. Fu, Y. C. Liu et al., "Structure-activity relationship studies of  $\beta$ -lactam-azide analogues as orally active antitumor agents targeting the tubulin colchicine site," *Scientific Reports*, vol. 7, no. 1, article 12788, 2017.
- [23] K. S. Sweetey, K. Nepali, S. Sapra et al., "Synthesis and biological evaluation of chalcones having heterosubstituent(s)," *Indian Journal of Pharmaceutical Sciences*, vol. 72, no. 6, pp. 801–806, 2010.
- [24] A. Masic, A. M. V. Hernandez, S. Hazra et al., "Cinnamic acid bornyl ester derivatives from valeriana wallichii exhibit antileishmanial in vivo activity in leishmania major-infected BALB/c mice," *Plos One*, vol. 10, no. 11, Article ID e0142386, 2015.
- [25] D. Tasdemir, M. Kaiser, R. Brun et al., "Antitrypanosomal and antileishmanial activities of flavonoids and their analogues: in vitro, in vivo, structure-activity relationship, and quantitative structure-activity relationship studies," *Antimicrobial Agents and Chemotherapy*, vol. 50, no. 4, pp. 1352–1364, 2006.
- [26] S. Kumar, B. K. Singh, P. Arya et al., "Novel natural product-based cinnamates and their thio and thiono analogs as potent inhibitors of cell adhesion molecules on human endothelial cells," *European Journal of Medicinal Chemistry*, vol. 46, no. 11, pp. 5498–5511, 2011.
- [27] D. Steverding, F. R. da Nóbrega, S. A. Rushworth, and D. P. de Sousa, "Trypanocidal and cysteine protease inhibitory activity of isopentyl caffeate is not linked in *Trypanosoma brucei*," *Parasitology Research*, vol. 115, no. 11, pp. 4397–4403, 2016.
- [28] J. R. Peterson, M. E. Russell, and I. B. Surjasasmita, "Synthesis and experimental ionization energies of certain (*E*)-3-arylpropenoic acids and their methyl esters," *Journal of Chemical and Engineering Data*, vol. 33, no. 4, pp. 534–537, 1988.
- [29] J.-C. Jung, S. Moon, D. Min, W. K. Park, M. Jung, and S. Oh, "Synthesis and evaluation of a series of 3,4,5-trimethoxycinnamic acid derivatives as potential antinarcotic agents," *Chemical Biology and Drug Design*, vol. 81, no. 3, pp. 389–398, 2012.
- [30] A. I. Vogel, A. R. Tatchell, B. S. Furniss, A. S. Hannaford, and P. W. G. Smith, *Practical Organic Chemistry*, Longman Scientific and Technical, Essex, UK, 1989.
- [31] B. Liu, A.-J. Deng, J.-Q. Yu, A.-L. Liu, G.-H. Du, and H.-L. Qin, "Chemical constituents of the whole plant of *elsholtzia rugulosa*," *Journal of Asian Natural Products Research*, vol. 14, no. 2, pp. 89–96, 2012.
- [32] J.-C. Jung, D. Min, H. Kim et al., "Design, synthesis, and biological evaluation of 3,4,5-trimethoxyphenyl acrylamides as antinarcotic agents," *Journal of Enzyme Inhibition and Medicinal Chemistry*, vol. 25, no. 1, pp. 38–43, 2009.
- [33] X.-D. Yang, X.-H. Zeng, Y.-H. Zhao et al., "Silica gel-mediated amide bond formation: an environmentally benign method for liquid-phase synthesis and cytotoxic activities of amides," *Journal of Combinatorial Chemistry*, vol. 12, no. 3, pp. 307–310, 2010.
- [34] J. G. H. Barajas, L. Y. V. Méndez, V. V. Kouznetsiv, and E. E. Stashenko, "Efficient synthesis of new *N*-Benzyl- or *N*-(2-furylmethyl)cinnamamides promoted by the 'Green' catalyst boric acid, and their spectral analysis," *Synthesis*, vol. 2008, no. 3, pp. 377–382, 2008.
- [35] X. Huang, X. Li, M. Zou et al., "From ketones to esters by a Cu-catalyzed highly selective C(CO)-C(alkyl) bond cleavage: aerobic oxidation and oxygenation with air," *Journal of the American Chemical Society*, vol. 136, no. 42, pp. 14858–14865, 2014.
- [36] B. Rivero-Cruz, I. Rivero-Cruz, R. Rodríguez-Sotres, and R. Mata, "Effect of natural and synthetic benzyl benzoates on calmodulin," *Phytochemistry*, vol. 68, no. 8, pp. 1147–1155, 2007.
- [37] D. C. Soares, C. G. Pereira, M. Â. A. Meireles, and E. M. Saraiva, "Leishmanicidal activity of a supercritical fluid fraction obtained from *Tabernaemontana catharinensis*," *Parasitology International*, vol. 56, no. 2, pp. 135–139, 2007.
- [38] S. A. Ahmed, R. M. Gogal, and J. E. Walsh, "A new rapid and simple non-radioactive assay to monitor and determine the proliferation of lymphocytes: an alternative to [3H]thymidine

- incorporation assay," *Journal of Immunological Methods*, vol. 170, no. 2, pp. 211–224, 1994.
- [39] P. C. D. Hawkins, *OMEGA OpenEye Scientific Software*, OMEGA, Santa Fe, NM, USA, 2010.
- [40] P. Tosco, T. Balle, and F. Shiri, "Open3DALIGN: an open-source software aimed at unsupervised ligand alignment," *Journal of Computer-Aided Molecular Design*, vol. 25, no. 8, pp. 777–783, 2011.
- [41] J. W. Ponder and F. M. Richards, "An efficient Newton-like method for molecular mechanics energy minimization of large molecules," *Journal of Computational Chemistry*, vol. 8, no. 7, pp. 1016–1024, 1987.
- [42] P. Tosco and T. Balle, "Open3DQSAR: a new open-source software aimed at high-throughput chemometric analysis of molecular interaction fields," *Journal of Molecular Modeling*, vol. 17, no. 1, pp. 201–208, 2010.





Hindawi

Submit your manuscripts at  
[www.hindawi.com](http://www.hindawi.com)

